Particle Transport with High Power Central ECH and ECCD in TCV

H. Weisen, I. Furno, T. Goodman and the TCV Team

Centre de Recherches en Physique des Plasmas
Association EURATOM-Confédération Suisse
École Polytechnique Fédérale de Lausanne
CH-1015 Lausanne, Switzerland

E-mail address of main author: Henri.Weisen@epfl.ch

Abstract. A coupled heat and particle transport phenomenon, leading to particle depletion from the plasma core is observed in a variety of plasma conditions with centrally deposited ECH and ECCD in TCV. This phenomenon, which causes inverted sawteeth of the central density in sawtoothing discharges and leads to stationary hollow profiles in the absence of sawteeth, has been linked to the presence of $m/n = 1/1$ MHD modes. In particular this phenomenon, known as "density pumpout" can be suppressed by stabilizing the mode by means of operation at high triangularity. The correlation of pumpout with the loss of axisymmetry suggests that neoclassical transport processes involving locally trapped particles near the helically displaced magnetic axis, previously believed to be important only in stellarators, may account for the phenomenon in tokamaks as well.

1. Introduction

ECH and ECCD are attractive candidate heating and current drive methods for future tokamak experiments, in particular ITER. However these methods appear to be at the origin of unexpected transport phenomena, which are potentially important for the confinement of fusion plasmas. In several past and present experiments, ECH is often seen to lead to a reduction of plasma particle density and confinement [1,2]. Such a phenomenon is also observed in stellarators, where it is at least qualitatively explained by neoclassical transport processes (thermodiffusion) arising from the presence of locally trapped particles due to the existence of magnetic field modulations throughout the plasma cross section [3]. Since the toroidal magnetic field ripple is very small on axis in most tokamaks, there are in principle no locally trapped particles in the core of axisymmetrical tokamaks. As a result the pumpout effect in tokamaks has remained unexplained.
The latest evidence from the TCV tokamak [4] (R_0=0.88m, a<0.25m, B_T<1.54T, I_p<1.2MA), which is currently equipped with 3 MW of ECH at the second harmonic (82.7GHz), suggests that pumpout in stellarators and in the core region of tokamaks is most probably of the same physical origin. Whereas in stellarators the field modulation is a built-in feature of the magnetic configuration, in tokamaks it can result from MHD perturbations caused by instabilities affecting the plasma core, especially inside the $q = 1$ surface. The presence of an $m/n = 1/1$ island causes the core to be helically displaced. As a result trapped particles exist even on the axis, just as in a heliac configuration. The coexistence of locally and toroidally trapped particles within the $q = 1$ surface can be expected to give rise to competing transport phenomena, including pumpout, since the off-diagonal terms associated with these two classes of particles have opposite signs.

2. Experimental evidence

Fig. 1 shows sawtooth oscillations using soft X-ray and interferometer signals in an ECH discharge with deposition outside (a) and inside (b) the sawtooth inversion radius r_{inv}. While deposition outside r_{inv} leads to sawteeth with positive ramps on both signals, deposition inside r_{inv} leads to negative density ramps (inverted sawteeth) in this low triangularity discharge (δ_{95}=0.22). The phenomenon is observed for $P_{ECH} > 0.5$ MW, as shown in Fig. 2 for Ohmic

and ECH phases of the same discharge. Fig. 3 shows the crash amplitudes $\Delta\bar{n}_{e0}/\bar{n}_{e0}$ from an ECH power scan for low and high triangularity obtained from a central line integrated electron density signal.

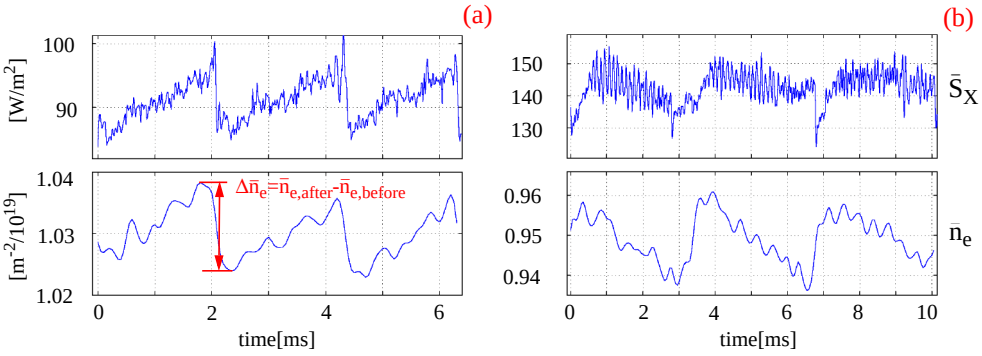

ig. 1 Discharge No. 16061. Sawtooth oscillations from a central line integrated soft X-ray hannel (top) and from a central interferometer channel (bottom), corresponding to ECH ower deposition outside (a) and inside (b) the sawtooth inversion surface.

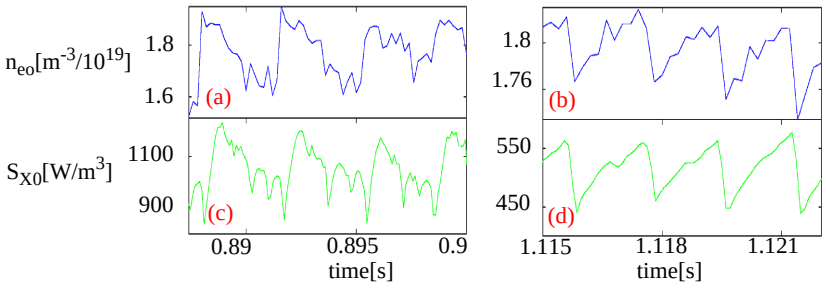

Fig. 2 Discharge No. 14475. Sawteeth at different injected ECH power from Abel-inverted central electron density (a, b) and on local soft X-ray emissivity (c, d).

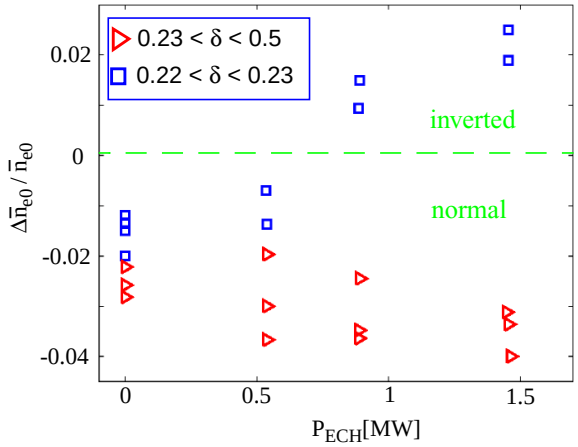

Fig. 3 Relative variation of $\bar{n}_{e0}$ at the sawtooth crash for different plasma triangularity and injected ECH power. Positive and negative $\Delta\bar{n}_{e0}/\langle\bar{n}_{e0}\rangle$ values indicate respectively inverted and normal sawteeth

At high triangularity no pumpout is observed. It is a generally observed feature in TCV, both in Ohmic [5] and ECH plasmas [6], that $m/n = 1/1$ pre-and postcursor oscillations are absent at high triangularity and are increasingly present as triangularity is reduced, suggesting a link between mode activity and the observed particle transport. Approximate heat and particle balance estimates for the plasma inside the sawtooth inversion radius show that the convectively expelled thermal energy during the inverted ramp phase is a small fraction, less than 10%, of the total loss power from that volume. In sawtoothing plasmas significantly hollow density profiles cannot develop because the crashes regularly flatten density and

temperature profiles. However with ECH and ECCD many situations arise when sawteeth are stabilized for long enough (typically 10 ms or more) for profiles to approach steady-state and the hollowness to become significant enough for measurements using the TCV Thomson scattering system. The absence of sawteeth is often accompanied by saturated $(1, 1)$ modes (as well as higher harmonics), indicating that the plasma still has a $q = 1$ surface. Fig. 4 shows typical examples of electron density in a fully sustained Co-ECCD and a Counter-ECCD discharge showing that the pumpout phenomenon is very general and does not depend on the parallel velocity of the electrons interacting with the heating beams.

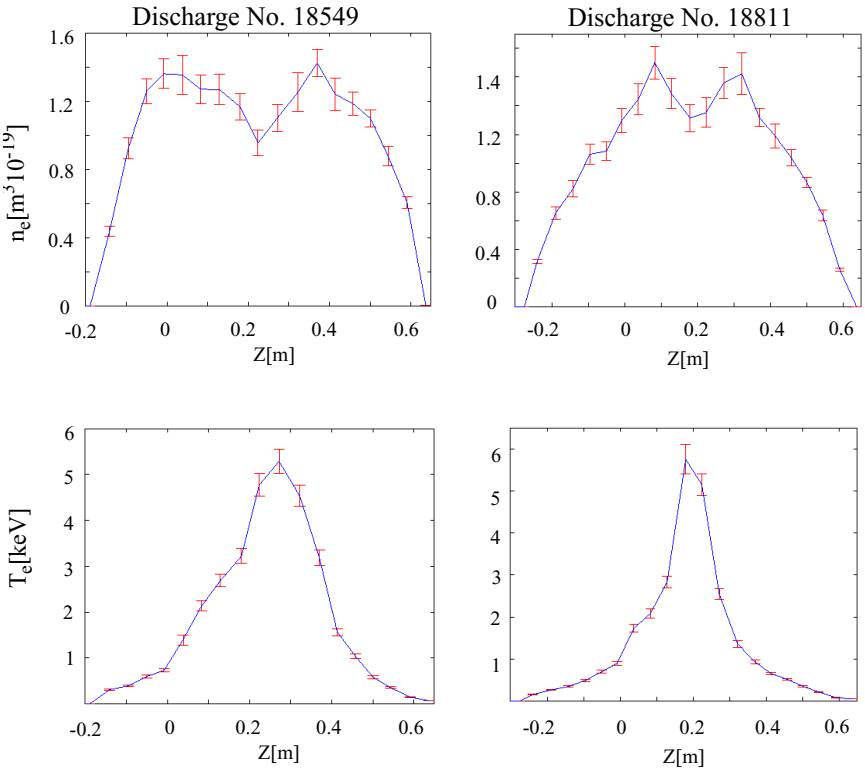

Fig. 4 Examples of electron density (top) and temperature (bottom) profiles in a Co-ECCD (left) and a Counter-ECCD discharge (right).

3. Discussion

Several explanations for "pumpout" have been suggested. Pondermotive effects are the least likely, both because the potentials are easily shown to be far smaller than electron temperatures and because the beams are very localized poloidally and toroidally, whilst the phenomenon is observed outside the beam region. In principle the thermal force [7] could transfer parallel momentum to ions in the presence of a parallel electron temperature gradient. Such an explanation might fit into the (controversial) picture of electron diffusion in stochastic magnetic fields, but would not make the economy of considering ion orbits. The first explanation based on particle orbits was proposed by Hsu et al [8]. According to this theory, the ECH, by increasing the perpendicular energy of electrons of low parallel velocity, causes many of these to become toroidally trapped, leading to the buildup of an excess of banana-electrons and thereby a poloidal charge asymmetry which produces a net electric field oriented in the direction of the major radius ("banana pile-up"). The resulting increased ion vertical drift velocity, by widening ion orbits, would then increase the neoclassical diffusivity and lead to increased particle losses.

The banana pile-up explanation however does not explain why pumpout is observed with heating on the high field side of the magnetic axis, which is the case in most TCV experiments, nor with large toroidal injection angles as are used for ECCD experiments, when the power is deposited to electrons with large $v_{/\!/}$. A model which only predicts increased diffusivities cannot

explain the observed gradient reversal. Finally banana pile-up cannot account for the observed importance of MHD modes.

We propose that loss of axisymmetry provides the crucial physics for this phenomenon by allowing the existence of locally trapped particles, which are not confined in the core region. Fig. 5 shows a schematic of the magnetic configuration inside the $q = 1$ surface when a magnetic island causes a helical displacement of the magnetic axis by a distance ξ. This displacement is typically of order 10% of the minor radius, as determined from X-ray tomography. The magnetic field modulation produced by the displacement inside the $q = 1$ surface is $\Delta B/B \cong \xi/R_0$. Particles with $|v_{//}/v|<(2\xi/R_0)^{1/2}$ on the low field side are not confined and can be expected to drift outside of the $q = 1$ volume where they find themselves in an (approximately) axisymmetrical field configuration and may remain confined as banana particles. Some of the particles escaping from the core region may also become trapped in the toroidal field ripple (which increases with distance from the core) and drift out of the plasma altogether.

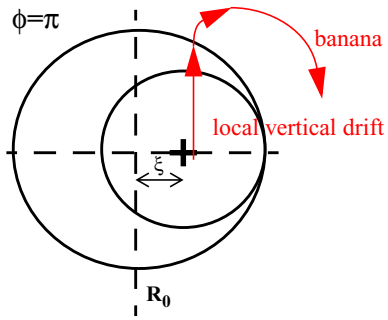

Fig. 5 Helically displaced plasma core and locally trapped particle orbit (schematic).

The nature of a configuration can be characterized by the parameter $\alpha = \varepsilon B/(\Delta B q n)$, where ε is the aspect ratio, q the safety factor and n the number of toroidal modulations [9]. For the configuration considered in Fig.5 $\alpha \cong \rho/\xi$. It is stellarator-like for $\rho < \xi$ and becomes increasingly like an ideal tokamak when $\rho > \xi$. In principle both collisions and direct perpendicular energy transfer by ECH can cause electrons to become trapped. Since pumpout occurs even with ECH on the high field side, where trapped electrons cannot be created directly, we must assume that collisional trapping is the most important of these mechanisms.

The vicinity of the displaced magnetic axis may act as a sink from where locally trapped particles are lost to beyond the non-axisymmetrical region (typically outside $q=1$). The coexistence of two classes of trapped particles may also give rise to competing transport phenomena. In neoclassical theory [9] trapped particles give rise to coupled heat and particle transport, of the generic form

$$\Gamma_{e,i} = D_{11}^{e,i} n_{e,i} \left[\left(\frac{n'_{e,i}}{n_{e,i}} + \frac{q Z_{e,i} \Phi'}{T_{e,i}} \right) + d_{12}^{e,i} \frac{T'_{e,i}}{T_{e,i}} \right] \qquad (1)$$

d_{12} giving rise to thermodiffusion (primes designate spatial derivatives). A steady state solution is obtained in the usual way by setting the ion flux to zero and inserting the ambipolar potential into the electron equation, with the result

$$\frac{n_e'}{n_e} = -d_{12}^e \left(1 + \frac{d_{12}^i T_i'}{d_{12}^e Z T_e'} \right) \Big/ \left(1 + \frac{T_i}{Z T_e} \right) \cdot \frac{T_e'}{T_e} \approx -d_{12}^e \frac{T_e'}{T_e} \qquad (2)$$

where the last approximation pertains to typical conditions on TCV, where $T_e >> T_i$. For fluxes caused by toroidally trapped particles we have $d_{12}^t = -0.5$, corresponding to an inward pinch, while for locally trapped particles $d_{12}^l \sim 1$ in the long mean free path regime and $d_{12}^l \sim 3.5$ in the $1/\nu$ regime [9], corresponding, for peaked temperature profiles, to an outward flux. In a realistic situation both processes as well as anomalous transport must be expected to compete. Formally we may write the total flux as a sum $\Gamma = \Gamma^t + \Gamma^l + \Gamma^a$, with $D_{11} = D_{11}^t + D_{11}^l + D_{11}^a$ and the superscript ^{a} refers to anomalous. The resulting off-diagonal term is then

$$d_{12} = (d_{12}^t \cdot D_{11}^t + d_{12}^l \cdot D_{11}^l + d_{12}^a \cdot D_{11}^a)/D_{11} \quad (3)$$

(Note that D_{11}^x may depend on electric fields). In the absence of an anomalous pinch, a hollow profile is expected where $D_{11}^l/D_{11}^t > -d_{12}^t/d_{12}^l \sim 0.5$, e.g. sufficiently close to the displaced axis. Fig. 6 shows the relations between the temperature and density gradients obtained in a variety of discharges including, Co- and Counter-ECCD. Although the results are qualitatively consistent with the existence of neoclassical outward fluxes due to locally trapped particles, the observed density gradients $\langle \nabla n_e \rangle / n_{e0} \sim -0.5 \cdot \langle \nabla T_e \rangle / T_{e0}$ in hollow profiles are smaller than expected from locally trapped particles alone. From Eq. (3) we see that the effect of anomalous diffusion, which generally can be expected to dominate, is to erode the strong steady-state gradients predicted by Eq. (2), which would be produced by neoclassical effects alone. We attribute the absence of strongly hollow profiles to the smallness of the stellarator-like region where local trapping dominates and to the competing effects of toroidal trapping and anomalous diffusion outside this region.

The above considerations should be regarded as tentative since it is not clear wether standard neoclassical theory can be applied. Locally trapped particle orbits for instance, even in the presence of electric fields, may well be larger than the stellarator-like region near the magnetic axis, as indicated in Fig.5. Clearly future work to test and refine the emerging physical picture of the pumpout phenomenon in tokamaks will require numerical orbit calculations and an improved understanding of neoclassical transport in the particular magnetic configurations which result when MHD instabilities break the symmetries of the ideal tokamak.

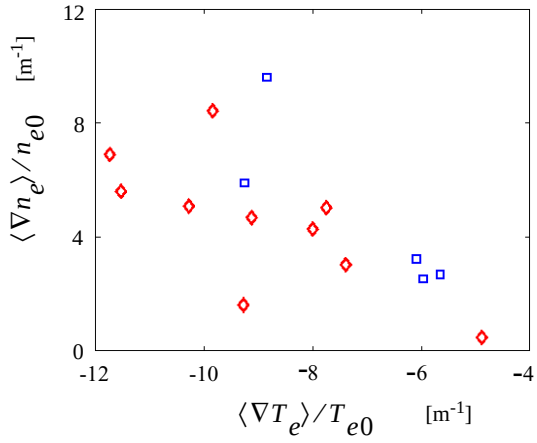

Fig. 6 Average electron density versus average T_e gradients over region with hollow n_e profiles.
squares: Co-ECCD
diamonds: Counter-ECCD

Acknowledgement: This work was partly supported by the Swiss National Science Foundation. The authors thank K. Lackner, H. Maassberg and W.A. Cooper for stimulating discussions.

References

[1] TFR-GROUP, *Nucl. Fusion* **25** (1985) 1011.
[2] V. Erckmann and U. Gasparino, *Plasma Phys. Control. Fusion* **36** (1994) 1862.
[3] H. Renner, W7-AS Team, NBI Group, ICF Group and ECRH Group, *Plasma Phys. Control. Fusion* **31** (1989) 1579.
[4] F. Hofmann, et al., *Plasma Phys. Control. Fusion* **36** (1994) B277.
[5] H. Weisen, et al., Nucl. Fusion **37** (1997) 1741.
[6] H. Reimerdes, et al., *Plasma Phys. Control. Fusion* **42** (2000) 629.
[7] Braginskii in Review of Plasma Physics **1**, Ed. M. A Leontovich (1965) 205
[8] J. Y. Hsu, at al., *Phys. Rev. Lett.* **53** (1984) 564.
[9] L. M. Kovrizhnykh, Nucl. Fusion **24** (1984) 851.